metals

Article

Thermal Wave Scattering and Temperature Concentration around the Opening in Platinum–Rhodium Leaky Plates

Weibo Jiang [1], Chuanping Zhou [1,2,*], Zhixian Yang [3], Zhi Sun [2], Huawei Ji [1], Ban Wang [1,4] and Qiaoyi Wang [1,5]

1 Key Laboratory of Mechanical Equipment and Technology for Marine Machinery, School of Mechanical Engineering, Hangzhou Dianzi University, Hangzhou 300018, China; jiangweibo2020@163.com (W.J.); jhw76@hdu.edu.cn (H.J.); bigban@zju.edu.cn (B.W.); wangqiaoyi1966@hotmail.com (Q.W.)
2 School of Mechatronic Engineering, China University of Mining and Technology, Xuzhou 221116, China; sunzhi@cumt.edu.cn
3 Wuxi Yintai Metal Products Co. Ltd, Wuxi 214194, China; yangzx1990@163.com
4 College of Electrical Engineering, Zhejiang University, Hangzhou 310027, China
5 The Department of Production Technology, University of Bremen, 28359 Bremen, Germany
* Correspondence: cpzhou0011@163.com; Tel.: +86 13429168099

Received: 20 May 2020; Accepted: 7 July 2020; Published: 14 July 2020

Abstract: Based on the non-Fourier heat conduction wave model, the thermal wave scattering near the opening in the platinum–rhodium glass fiber leaky plate structure is studied by using complex function method and conformal mapping method, and the general solution of the thermal wave scattering problem is given. The boundary condition of the open surface is adiabatic. The influence of the geometrical and physical parameters of the leaky plate on the temperature distribution in the plate is analyzed, and the numerical results of the temperature concentration are given. This study can provide theoretical basis and reference data for the design and optimization of the opening structure of platinum–rhodium glass fiber leaky plate.

Keywords: platinum–rhodium leaky plate; non-Fourier thermal conductivity; thermal wave scattering; opening; temperature concentration

1. Introduction

Platinum–rhodium alloy material has high temperature resistance, corrosion resistance and oxidation resistance, which is used to process glass fiber in engineering manufacturing. There are a lot of small openings on the platinum–rhodium glass fiber leaky plate (Pt–Rh GFLP). Under the action of high temperature molten liquid in the low stress oxidation environment for a long time, the temperature rises rapidly, which inevitably causes the oxidation volatilization of Pt–Rh GFLP. The stress concentration and temperature field concentration appear near the opening. The bearing capacity decreases, and the service life shortens. Therefore, the research on the temperature field in the vulnerable area of the Pt–Rh GFLP under the extremely fast heating environment is in urgent need of theoretical research as an engineering reference.

Since Fourier established the mathematical model of heat conduction in the 19th century, Fourier law has been widely used in various fields of heat conduction problem analysis. For the steady-state heat transfer process with long thermal action time, the Fourier law can be used to describe the relationship between heat flow density and temperature gradient, which can meet the accuracy requirements [1–3]. However, Fourier's law implies the assumption that the propagation speed of thermal disturbance is large and does not involve the time term of heat transfer, so it is no longer applicable to the problem of heat conduction in the extremely fast heating environment of Pt–Rh GFLP [4–8]. In order to overcome the limitation of Fourier law, Cattaneo and Vernote independently proposed a non-Fourier heat conduction model with heat flow delay phase, taking into account the influence of heat flow change rate on heat conduction [4]. Sarkar and Haji Sheikh [5] studied the hyperbolic heat conduction problem of finite plates made of dielectric materials by Laplace transformation. Barletta and Zanchini [7] analyzed the hyperbolic heat conduction problem of large cylinder with internal heat source and heat convection with external fluid. Tang and Araki [8] solved the non-Fourier heat conduction problem of a finite medium under periodic surface heating. Moosaie [9] studied the non-Fourier heat conduction problem of solid-state lasers by numerical simulation. Atefi and Talaee [10] solved the non-Fourier temperature field of a large cylinder with boundary conditions that did not change with time by using the separation variable method. Mishra and Sahai [11] use lattice Boltzmann method to study the non-Fourier heat conduction problem of one-dimensional cylinder and sphere. Ma et al. [12] got a general solution of the scattered field of thermal waves from the cylindrical subsurface inclusion in the large plate. Zhang et al. [13] studied a thermal shock problem of an elastic strip made of functionally graded materials based on the fractional heat conduction theory. Niwa et al. [14] studied the high-temperature bending fatigue properties of oxide dispersion-strengthened platinum–rhodium alloy under high axial stress. Sellitto et al. [15] presented generalized heat-conduction laws from a mesoscopic perspective and studied mesoscopic theories of heat transport in nanosystems. Machrafi [16] provided for a systematic presentation of extended non-equilibrium thermodynamics in nanosystems with a high degree of applicability. Jou et al. [17] studied the formulation of extended irreversible thermodynamics within the framework of the rational thermodynamics. Cimmelli [18] present an overview of the modern approaches to continuum nonequilibrium thermodynamics from the perspective of their connection with the problem of heat conduction with finite speed.

The thermal wave theory (Cattaneo–Vernotte equation) and Boltzmann method were investigated in the above literature [5–11]. According to these studies we have the following views on the Cattaneo–Vernotte model (CV model). One question is the compatibility of the CV equation with the second law of thermodynamics. For the CV model allows heat flow from low temperature to high temperature, it is easy to be considered that the CV model violates the second law of thermodynamics. However, in fact the case of deviation from equilibrium is dealt with in the CV model. The entropy of the system depends not only on the properties of equilibrium states such as temperature, but also on some other parameters such as the heat flux. This is one of the basic understandings of the extended thermodynamics. On this basis, it can be proved that the entropy produced by the thermal wave theory such as the CV model is non-negative [19]. Therefore, the thermal wave model such as the CV model is compatible with the basic principles of the second law of thermodynamics. The essence of this question is that the CV model is mistakenly put under the conceptual framework of the equilibrium continuum model. In fact, the CV model can only be built on the conceptual framework of extended thermodynamics. Besides, the Boltzmann transfer equation (BTE) is compared with the thermal wave theory in reference [19]. In the thermal wave theory, the nonlocality in time is generally considered and the nonlocality in space is generally ignored. BTE considers both temporal and spatial nonlocality. Considering a gas system with large thermal relaxation time [19,20], if only time nonlocality is retained, the system will lose the space transport completely, and it will be only related with time, which is totally inconsistent with the actual situation. This shows that the spatial nonlocality cannot be ignored, and the thermal wave theory cannot be applied in the gas system with large thermal relaxation time. In this paper, the research object is metallic material, and its thermal relaxation time is finite, so the CV model is generally applicable.

In engineering practice, the Pt–Rh GFLP is heated by ultrashort laser pulse. By controlling the frequency which refers to the periodic repetition of laser pulses and amplitude of the ultrashort laser pulse, the temperature field near the opening of the Pt–Rh GFLP can be measured, and the subsurface microstructure information of the platinum rhodium alloy material can be obtained, so as to realize the optimal design of the opening structure of the Pt–Rh GFLP. In this paper, the problem of thermal wave scattering and surface temperature distribution in a Pt–Rh GFLP structure based on the wave equation of non-Fourier heat conduction is studied, and the effects of various physical parameters on temperature distribution is analyzed. The analysis in this paper is of great significance for solving the problem of concentrated temperature distribution near openings or defects in various metal plates at extremely high temperatures.

2. Wave Equation of Heat Conduction and Its General Solution

The research object is a Pt–Rh GFLP with a circular opening and a large length in the x direction as shown in Figure 1. A thermal wave process can be formed inside the material as a laser pulse beam with a modulation frequency of f irradiated on the outer surface of the leaky plate. The boundary conditions of the Pt–Rh GFLP are that the upper, lower, front, and rear boundary plane are all constant temperature surfaces equal to the ambient temperature. The boundary conditions of the left and right ends of the Pt–Rh GFLP are not discussed here for the longitudinal length of the plate is large. Because of the small area of the opening wall, it is very difficult to exchange heat with the outside world, so it is treated as an adiabatic surface in the paper. At the same time, suppose the temperature field distribution in the z-direction is uniform, which means the problem of two-dimensional temperature field in the coordinate (x,y) is studied.

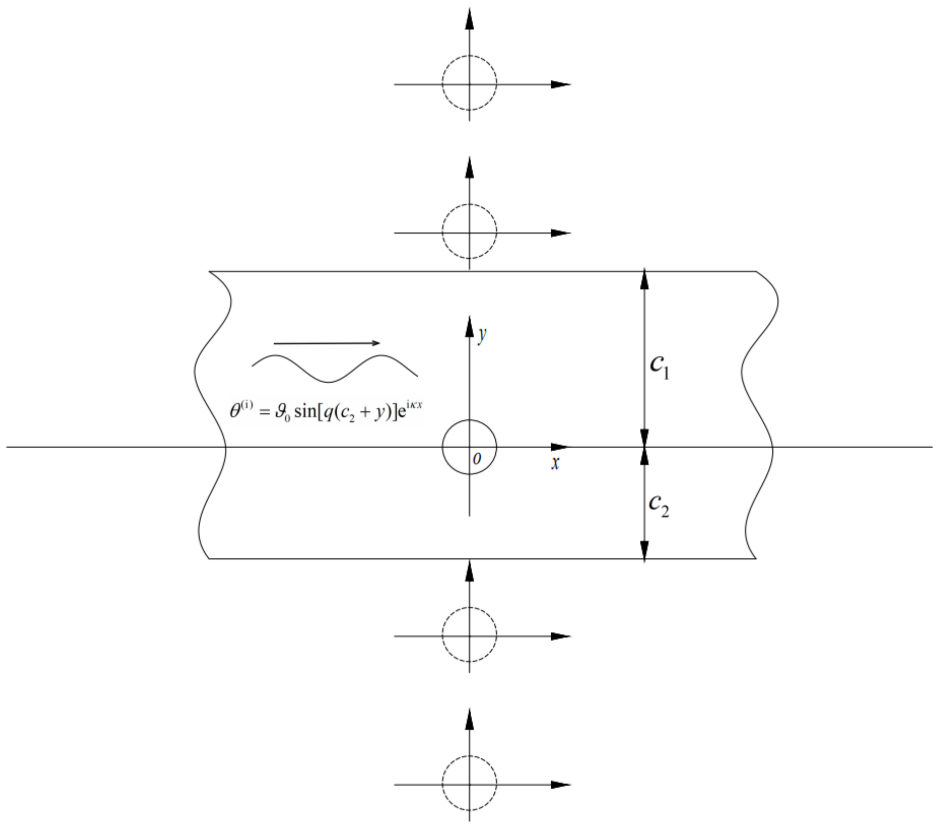

Figure 1. Diagram of Pt–Rh glass fiber leaky plate structure with a circular opening under pulse heating.

The temperature governing equation in the solid medium without internal heat source can be obtained according to the non-Fourier heat conduction equation [21].

$$\nabla^2 T = \frac{1}{c^2}\frac{\partial^2 T}{\partial t^2} + \frac{1}{D}\frac{\partial T}{\partial t} \quad (1)$$

where ∇^2 is Laplace operator, $\nabla^2 = \frac{\partial^2}{\partial x^2} + \frac{\partial^2}{\partial y^2}$; λ, c_p, ρ are respectively the thermal conductivity, specific heat capacity at constant pressure and density; $D = \lambda/\rho\, c_p$ is the thermal diffusivity; $c = \sqrt{D/\tau}$ is the thermal wave propagation speed; τ is the thermal relaxation time; T is the temperature in the Pt–Rh GFLP. The density of platinum–rhodium 5% alloy leaky plate and platinum–rhodium 10% alloy leaky plate are taken ρ = 21 g/cm^3 and ρ = 20.5 g/cm^3 respectively; The thermal conductivity of platinum–rhodium 5% alloy leaky plate and platinum–rhodium 10% alloy leaky plate measured by Wuxi Yintai Metal Products Co. Ltd are respectively λ = 69.9 W/(m·K) and λ = 70.05 W/(m·K). The difference of thermal conductivity between platinum–rhodium 5% and platinum–rhodium 10% is very small, and have little effect on the numerical calculation results, therefore, they are treated as equal in their thermal conductivity in the paper, taken λ = 70 W/(m·K) here. The specific heat capacity at constant pressure c_p = 0.133 KJ/(Kg·K) The thermal relaxation time $\tau = 10^{-12}$ s.

For a wave problem, the analytical solution can be divided into two types: time domain solution and frequency domain solution. And the two types can be converted to each other through Fourier transform method. For the internal flaw detection and detection of materials, it is necessary to use a periodic heat load to implement thermal incentives to make use of the phase and amplitude of the thermal echo, as well as the wave number and spatial attenuation coefficient, to determine the position, orientation and size of the openings in the material.

According to the Fourier decomposition theorem, the periodic heat conduction process can be regarded as the superposition of several simple harmonic motions. Therefore, the periodic non-steady-state heat conduction of the problem can be studied according to the normative analysis format of the wave theory.

Study the periodic non-steady-state heat conduction solution of Equation (1), assuming the expression of the temperature field is

$$T(x,y) = T_m + \mathrm{Re}[\vartheta \exp(-\mathrm{i}\omega\,\mathrm{t})] \tag{2}$$

Among them, the temperature amplitude should satisfy the Helmholtz equation of the following form

$$\nabla^2\vartheta + \kappa^2\vartheta = 0 \tag{3}$$

where Re means taking the real part; T_m is the average temperature of the environment; Excess temperature amplitude $\vartheta = T_{\max} - T_m$; ∇^2 is the Laplace operator, $\nabla^2 = \partial^2/\partial x^2 + \partial^2/\partial y^2$; ω is the circular frequency; κ is the complex wave number, $\kappa = \left(\frac{\omega^2}{c^2} + \mathrm{i}\frac{\omega}{D}\right)^{1/2} = \alpha + \mathrm{i}\beta$; $\mathrm{i} = \sqrt{-1}$ is the imaginary unit; α, β are respectively the thermal wave number and absorption coefficient, taking $\alpha > 0$, $\beta > 0$, after normalization, that is

$$\alpha = \sqrt{\frac{1}{2}\left[\sqrt{\frac{\omega^4}{c^4} + \frac{\omega^2}{D^2}} + \frac{\omega^2}{c^2}\right]} = \sqrt{\sqrt{\frac{1}{4}\kappa^2 + \frac{1}{\mu^4}} + \frac{1}{2}\kappa^2} \tag{4}$$

$$\beta = \sqrt{\frac{1}{2}\left[\sqrt{\frac{\omega^4}{c^4} + \frac{\omega^2}{D^2}} - \frac{\omega^2}{c^2}\right]} = \sqrt{\sqrt{\frac{1}{4}\kappa^2 + \frac{1}{\mu^4}} - \frac{1}{2}\kappa^2} \tag{5}$$

where k is the thermal wave number, $k = \omega/c$ when there is no diffusion effect, μ is the thermal diffusion length.

Using complex variable function method, introducing complex variables

$$\eta = x + \mathrm{iy},\ \overline{\eta} = x - \mathrm{iy} \tag{6}$$

Then

$$x = \frac{1}{2}(\eta + \overline{\eta}),\ y = \frac{1}{2\mathrm{i}}(\eta - \overline{\eta}) \tag{7}$$

Equation (3) can be transformed into the following form

$$\frac{\partial^2 \vartheta}{\partial \eta \partial \overline{\eta}} + \left(\frac{\kappa}{2}\right)^2 \vartheta = 0 \tag{8}$$

The general solution of the thermal wave scattering field of an opening in a Pt–Rh GFLP determined by Equation (3) is

$$\vartheta = \sum_{n=-\infty}^{\infty} A_n H_n^{(1)}(\kappa r) \mathrm{e}^{\mathrm{i}n\theta} = \sum_{n=-\infty}^{\infty} A_n H_n^{(1)}(\kappa|\eta|) \left\{ \frac{\eta}{|\eta|} \right\}^n \tag{9}$$

where A_n is the mode coefficient of the scattered wave generated by the circular opening in the leaky plate, which is determined by the boundary conditions; $H_n^{(1)}(\cdot)$ is the Hankel function of the first kind.

The conformal mapping method can be used to meet the boundary conditions of the circular openings when solving the wave scattering plane problem of openings of any shape in solids. The mapping function of the non-circular opening boundary on the η-plane to the unit circle boundary on the ζ-plane can be taken as [10,11]

$$\eta = \Omega(\zeta) \tag{10}$$

Giving proper mapping function, Equation (10) can be applied with openings of any shape, such as openings of triangular or rectangular cross section, etc. At this time, there may be $\eta = r\mathrm{e}^{\mathrm{i}\varphi}$ on the η-plane. The coordinates of any point can be expressed as $\zeta = R\mathrm{e}^{\mathrm{i}\theta}$ when taking Polar coordinates on the ζ-plane. In this way, the general solution of the non-circular opening thermal wave scattering field in the η-plane can be described as

$$\vartheta = \sum_{n=-\infty}^{\infty} A_n H_n^{(1)}\left(\kappa|\Omega(\zeta)|\right) \left\{ \frac{\Omega(\zeta)}{|\Omega(\zeta)|} \right\}^n \tag{11}$$

For an elliptical opening with a long axis and a half axis of a r_1 and r_2, the conformal mapping function can be taken as

$$\eta = \Omega(\zeta) = \frac{a}{1+\varepsilon}\left(\zeta + \frac{\varepsilon}{\zeta}\right) \tag{12}$$

where $a = \frac{1}{2}(r_1 + r_2), \varepsilon = \frac{r_1 - r_2}{r_1 + r_2}$.

3. Excitation of the Incident Wave and Total Wave Field

Assume that an ultrashort laser pulse source is heated at the left side of the Pt–Rh GFLP, and the temperature wave propagates in the positive x-direction. Based on the constructive interference theory of the wave field, the expression of the temperature distribution in the Pt–Rh GFLP can be set as

$$\vartheta = f(y)\exp(\mathrm{i}px) \tag{13}$$

This solution must satisfy the wave Equation (3), and the following expression can be obtained

$$f(y) = A\cos(qy) + B\sin(qy) \tag{14}$$

Where p and q are respectively the longitudinal wave number and the transverse wave number of temperature fluctuation, $p^2 = \kappa^2 - q^2$.

At the same time, the temperature boundary conditions of the upper and lower surfaces are

$$f(c_1)\exp(\mathrm{i}px) = 0,\ f(-c_2)\exp(\mathrm{i}px) = 0 \tag{15}$$

In this way, the transverse wave number of temperature fluctuation can be obtained as

$$q = \frac{n\pi}{c_1 + c_2}(n = 0, 1, 2 \cdots \infty) \tag{16}$$

Substituting Equation (16) into Equation (18), the expression of temperature distribution in the leaky plate can be obtained

$$\vartheta = B\frac{\sin[q(c_2 + y)]}{\cos(qc_2)}\exp[\mathrm{i}(px - \omega t)] \tag{17}$$

The thermal wave can be described as

$$\vartheta^{(i)} = \vartheta_0 \sin[q(c_2 + y)]\mathrm{e}^{\mathrm{i}px - \omega t} = \vartheta_0 \sin[q(c_2 + y)]\sum_{n=-\infty}^{\infty}\mathrm{i}^n J_n(pr)\mathrm{e}^{\mathrm{i}\,n\,\theta}\mathrm{e}^{-\mathrm{i}\,\omega\,t} \tag{18}$$

where ϑ_0 is the temperature amplitude of incidence thermal wave, i.e., excess temperature $\vartheta_0 = T_0 - T_m$; $q = \pi/(c_1 + c_2)$; p is the wave number along the x-direction; $J_n(\bullet)$ is the Bessel function. Correspondingly, under the adiabatic condition, the thermal wave can be described as

$$\vartheta^{(i)} = \vartheta_0 \cos[q(c_2 + y)]\mathrm{e}^{\mathrm{i}px}\,\mathrm{e}^{-\mathrm{i}\omega t} \tag{19}$$

Taking the multiple scattering by the solid boundary when $y = c_1$ and $y = c_2$ ($c_1 > 0$, $c_2 > 0$) for considerations, the scattered field of thermal waves by noncircular hole can be described in the Polar coordinates system as

$$\vartheta^{(s)} = \sum_{n=-\infty}^{\infty} A_n H_n^{(1)}(\kappa r)\mathrm{e}^{\mathrm{i}n\varphi} + \sum_{m=1}^{\infty}\sum_{n=-\infty}^{\infty} A_n H_n^{(1)}(\kappa r_m)\mathrm{e}^{\mathrm{i}n\,\varphi_m} \tag{20}$$

By the means of complex function method, Equation (21) can be simplified as

$$\begin{aligned}\vartheta^{(s)} = {} & \sum_{n=-\infty}^{\infty} A_n H_n^{(1)}(\kappa|\eta|)\left\{\frac{\eta}{|\eta|}\right\}^n + \sum_{n=-\infty}^{\infty} A_n\left\{\sum_{m=1}^{\infty}(-1)^1\left[H_n^{(1)}(\kappa|\eta - \eta_{1m}|)\left\{\frac{\eta-\eta_{1m}}{|\eta-\eta_{1m}|}\right\}^{(-1)n}\right]\right. \\ & + \sum_{m=1}^{\infty}(-1)^2\left[H_n^{(1)}(\kappa|\eta - \eta_{2m}|)\left\{\frac{\eta-\eta_{2m}}{|\eta-\eta_{2m}|}\right\}^{(-1)^2 n}\right] + \sum_{m=1}^{\infty}(-1)^3\left[H_n^{(1)}(\kappa|\eta - \eta_{3m}|)\left\{\frac{\eta-\eta_{3m}}{|\eta-\eta_{3m}|}\right\}^{(-1)^3 n}\right] \\ & \left. + \cdots + \sum_{m=1}^{\infty}(-1)^l\left[H_n^{(1)}(\kappa|\eta - \eta_{lm}|)\left\{\frac{\eta-\eta_{lm}}{|\eta-\eta_{lm}|}\right\}^{(-1)^l n}\right]\right\}\end{aligned} \tag{21}$$

For the convenience of calculation, we take $l = 4$, the scattered field of thermal wave field can be described as

$$\vartheta^{(s)} = \sum_{n=-\infty}^{\infty} A_n H_n^{(1)}(\kappa|\eta|)\left\{\frac{\eta}{|\eta|}\right\}^n + \sum_{n=-\infty}^{\infty} A_n \sum_{l=1}^{4}\sum_{m=1}^{\infty}(-1)^l H_n^{(1)}(\kappa|\eta - \eta_{lm}|)\left\{\frac{\eta - \eta_{lm}}{|\eta - \eta_{lm}|}\right\}^{(-1)^l n} \tag{22}$$

where, $\eta_{1m} = \mathrm{i}2(mL - c_2)$, $\eta_{2m} = \mathrm{i}2mL$, $\eta_{3m} = -\mathrm{i}2[(m-1)L + c_2]$, $\eta_{4m} = -2\mathrm{i}mL$; $L = c_1 + c_2$; $m = 1, 2, \cdots\infty$; $\exp(\mathrm{i}\varphi) = \Omega(\zeta)/|\Omega(\zeta)|$, $r = |\Omega(\zeta)|$, $\eta = \Omega(\zeta)$, $\eta' = \Omega'(\zeta)$.

Consequently, the total wave field is composed of the incidence and scattering field, which is conveyed by Equation (22)

$$\vartheta^{(t)} = \vartheta^{(i)} + \vartheta^{(s)} \tag{23}$$

According the Dirichlet boundary condition of heat conduction, the mode coefficient of the scattered wave A_n can be derived. In the calculation, the mode coefficients of scattered waves are truncated, and the algebraic equations to determine the mode coefficients are obtained.

4. Numerical Examples

The thermal wave scattering and surface temperature distribution of elliptical opening in Pt–Rh GFLP are calculated in order to show the effectiveness of the analysis and calculation method in this paper. The radius of the circular opening is $a = 1.0$ mm. The amplitude of the pulse mentioned below is 1270 °C.

Figure 2 correspond to the position of the circular opening along the transversal direction of the leaky plate, that is, in the y-direction: distance from the upper boundary is taken $c_1 = 200$ mm, distance from the lower boundary is taken $c_2 = 200$ mm; The laser pulse frequency is taken $f = 80$ Hz, $f = 160$ Hz, $f = 240$ Hz respectively; The mass fraction of rhodium element in Pt–Rh GFLP is 5%. Figure 2a shows the temperature distribution in the section $y \in (-30$ mm, 30 mm) with the center of the circular opening as the origin, and Figure 2b shows the temperature distribution in the section $y \in (-1.5$ mm, 1.5 mm) with the center of the circular opening as the origin. From the consistent trend of the three temperature distribution curves, it can be found that the temperature peaks at $y = 0$ position, and the temperature begins to increase suddenly in the section near $y \in (-0.5$ mm, 0.5 mm). The temperature gradually decreases as the distance from position increases, and the temperature distribution is symmetrical along the line $y = 0$. From the comparison of the differences in the three temperature distribution curves, as the laser pulse frequency increases, the peak temperature gradually decreases, and the length of section where the temperature suddenly increases gradually decreases; In the section other than $y \in (-1.5$ mm, 1.5 mm), the laser pulse frequency has no obvious influence on the distribution of temperature.

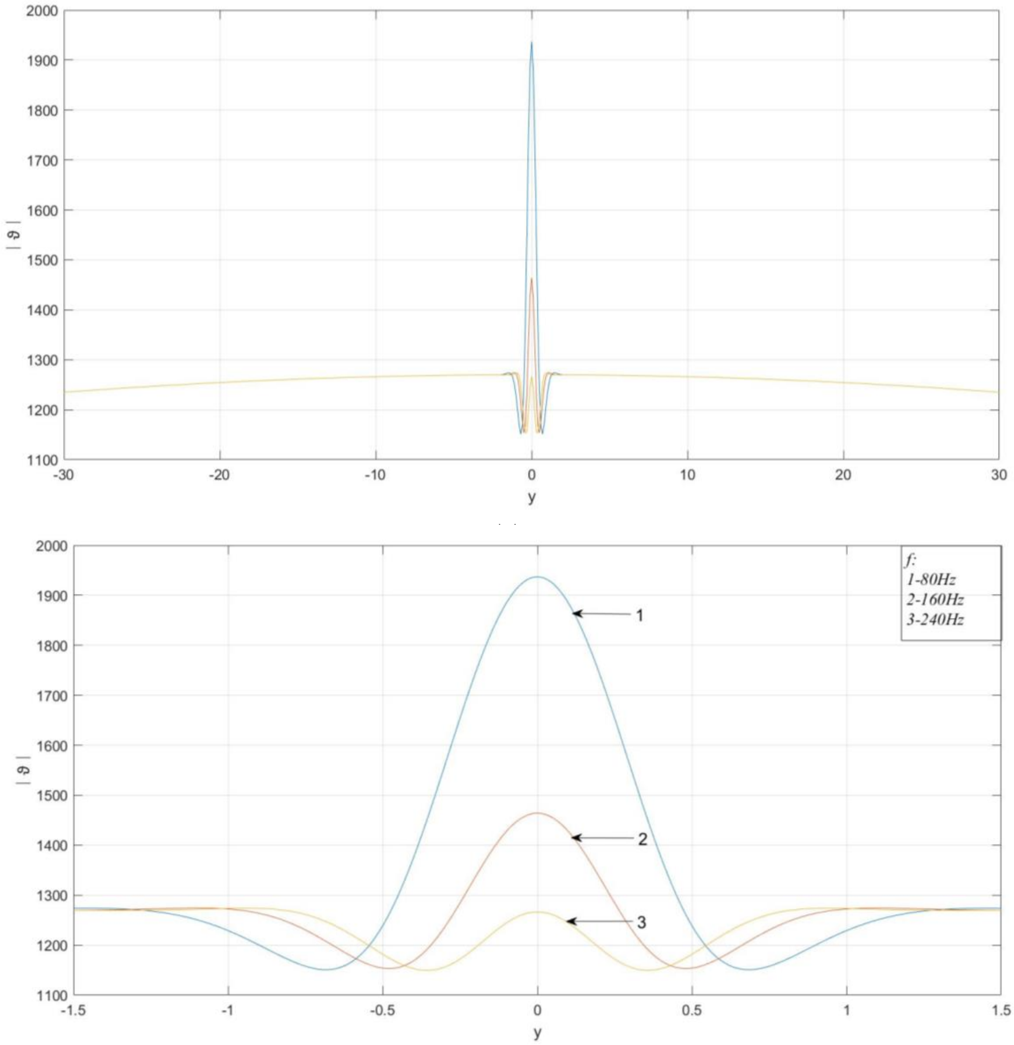

Figure 2. (**a**) Temperature near the circular opening of Pt–Rh GFLP, (**b**). Temperature near the circular opening of Pt–Rh GFLP.

Figure 3 correspond to the position of the circular opening along the transversal direction of the leaky plate, that is, the y-direction: distance from the upper boundary is taken c_1 = 200mm, distance from the lower boundary is taken c_2 = 200mm; The laser pulse frequency is taken f = 80 Hz; The mass fraction of rhodium element in Pt–Rh GFLP is taken 5% and 10% respectively. Figure 3a shows the distribution of temperature in the section $y \in$ (−30 mm, 30 mm) with the center of the circular opening as the origin, and Figure 3b shows the distribution of temperature in the section $y \in$ (−1.5 mm, 1.5 mm) with the center of the circular opening as the origin. From the consistent change trend of the two temperature distribution curves, it can be found that the temperature peaks at y = 0 position, and the temperature starts to increase suddenly in the section of $y \in$ (−0.7 mm, 0.7 mm), the temperature gradually decreases with the increase of the distance from y = 0 position, and the temperature distribution is symmetrical along the line y = 0. From the comparison of the differences in the three temperature distribution curves, as the laser pulse frequency increases, the peak temperature gradually decreases, and the length of section where the temperature suddenly increases gradually decreases; In the section other than $y \in$ (−1.5 mm, 1.5 mm), the laser pulse frequency has no obvious influence on the distribution of temperature.

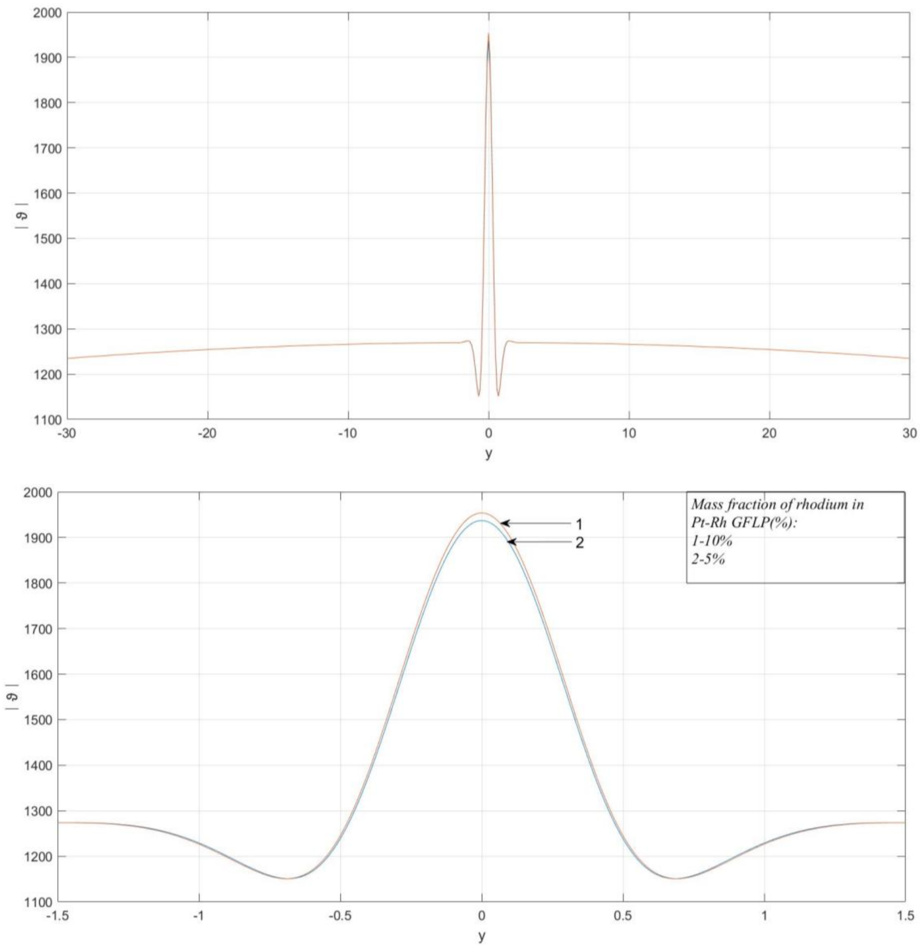

Figure 3. (**a**) Temperature near the circular opening of Pt–Rh GFLP, (**b**) Temperature near the circular opening of Pt–Rh GFLP.

Figure 4 correspond to the position of the circular opening along the transversal direction of the leaky plate, that is, the y-direction: distance from the upper boundary is taken c_1 = 100 mm, distance from the lower boundary is taken c_2 = 100 mm, c_2 = 150 mm, c_2 = 200 mm, c_2 = 250 mm respectively; The laser pulse frequency is taken f = 80 Hz; The mass fraction of rhodium element in Pt–Rh GFLP is 5%. Figure 4a shows the distribution of temperature in the section $y \in$ (−2 mm, 2 mm) with the center of the circular opening as the origin, and Figure 4b shows the distribution of temperature in the section $y \in (-c_1, c_2)$ with the center of the circular opening as the origin. It can be found from Figure 4b that when $c_2 \geq c_1$, the larger the c_2, the lower the peak temperature. Combining curve 3, it can be found that the temperature in the section $y \in (-100$ mm, -50 mm$)$ is increasing, the temperature in the section $y \in (-50$ mm, -1.5 mm$)$ is decreasing, and the temperature in the section $y \in (1.5$ mm, 100 mm$)$ is decreasing. This is different from the case where the temperatures of the first two groups are symmetrically distributed along the line $y = 0$. This is caused by the different distance of the circular opening from the upper and lower boundaries of the leaky plate. In the state without openings, the line $y = -50$mm is the center line of the transversal direction of the leaky plate, that is, the y-direction, when the leaky plate is heated by the laser pulse, the center line is the farthest from the boundary of the leaky plate, and has the least heat exchange with the outside environment, so its temperature is high; in the state with a circular opening, because the line $y = 0$ contains the center of the circular opening, the temperature suddenly increases when heated by the laser pulse, so there is a prominent part of the temperature in the figures. It can be found from Figure 4a that there is no significant difference in the temperature at the center line of the y-direction when c_2 is different. According to the rules found in Figure 4a,b, the opening center can be set reasonably outside the center line of the y-direction on the Pt–Rh GFLP to avoid overheating at the circular opening of the leaky plate due to the superposition of factors such as difficulty in heat dissipation at the center of the leaky plate and sudden temperature increase at the circular opening of the leaky plate.

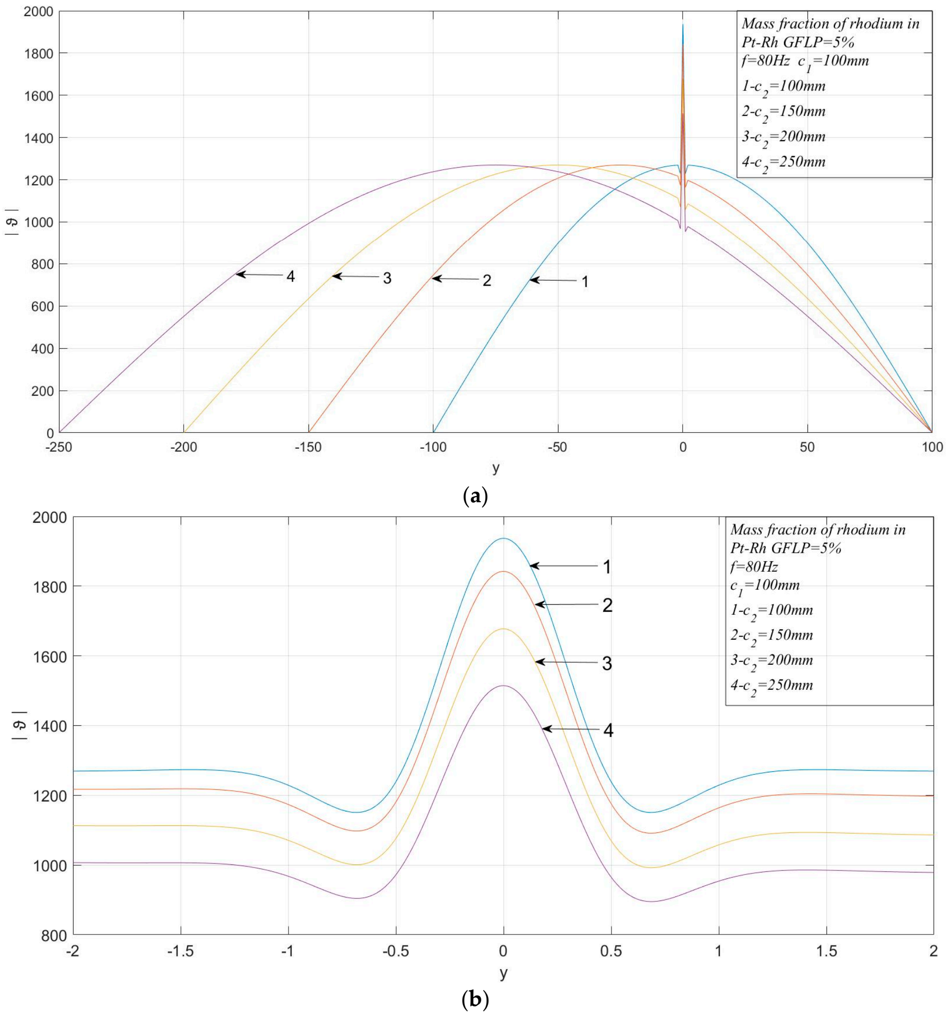

Figure 4. (**a**) Temperature near the circular opening of Pt–Rh GFLP (**b**). Temperature near the circular opening of Pt–Rh GFLP.

Figure 5 corresponds to the position of the circular opening along the transversal direction of the leaky plate, that is, the y-direction: distance from the upper boundary is taken $c_1 = 100$ mm, $c_1 = 200$ mm respectively, distance from the lower boundary is taken $c_2 = 100$ mm, $c_2 = 200$ mm respectively; The laser pulse frequency is taken $f = 80$ Hz; The mass fraction of rhodium element in Pt–Rh GFLP is from 0 to 30%. According to the data measured by Wuxi Yintai Metal Products Co. Ltd, during the process of the mass fraction of rhodium in the Pt–Rh GFLP changing from 0% to 30%, the changes of specific heat capacity and thermal conductivity are very small, and have little effect on the numerical calculation results, so they are treated as equal in the paper. The density of platinum–rhodium n% is 21.45 g/cm^3 $\times$ $(100 - n)$% + 12.41 g/cm^3 $\times$ n%. Figure 5 shows the temperature at the center of the circular opening, that is, the position of $y = 0$. It can be found from the Figure 5 that as the mass fraction of rhodium element in Pt–Rh GFLP increases, the temperature at the center of the circular opening gradually increases. The temperature at the circular opening is higher when $c_1 = c_2$, and in the case of $c_1 = c_2$, the temperature is always equal. The temperature is lower when $c_1 \neq c_2$.

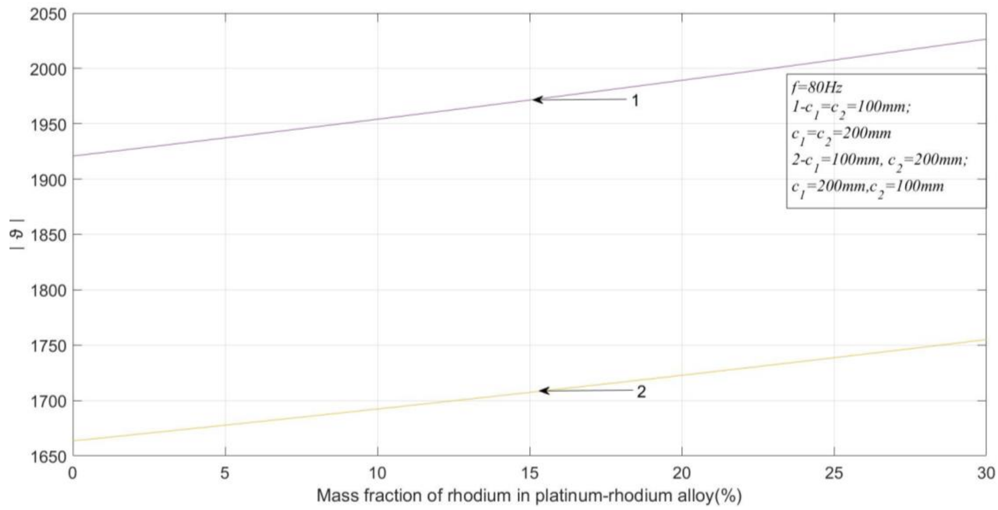

Figure 5. Temperature at the center of the circular opening of the Pt–Rh GFLP.

Figure 6 corresponds to the position of the circular opening along the transversal direction of the leaky plate, that is, the y-direction: distance from the upper boundary is taken $c_1 = 100$ mm, $c_1 = 200$ mm respectively, distance from the lower boundary is taken $c_2 = 100$ mm, $c_2 = 200$ mm respectively; The mass fraction of rhodium element in Pt–Rh GFLP in Figure 5 is 5%; The pulse frequency is taken from $f = 0.1$ Hz to $f = 300$ Hz. Figure 6 shows the temperature at the center of the circular opening, that is, the position of $y = 0$. It can be found from Figure 6 that when the frequency is in the section (0 Hz, 5 Hz), the temperature at the center of the circular opening increases with increasing frequency, and in the section (5 Hz, 300 Hz), the temperature at the center of the circular opening gradually decreases and tends to be stable with the increase of frequency. The temperature at the circular opening is higher when $c_1 = c_2$, and in the case of $c_1 = c_2$, the temperature is always equal. The temperature is lower when $c_1 \neq c_2$. We can see that in Figure 6 with a peak temperature value at about 5 Hz excitation. A reasonable explanation is that thermal wave behavior is similar to elastic waves in solid mechanics or acoustic waves in physics. The wave equation or vibration equation in dynamics is a hyperbolic equation. When the external excitation is close to the natural frequency of the system, dynamic stress concentration or resonance will occur with well-pronounced amplitude at a certain frequency. The heat conduction equation in this paper is also a hyperbolic equation, so it is reasonable to produce well-pronounced temperature excess amplitude within a certain thermal excitation frequency range. It provides an important theoretical reference for us to control the maximum temperature of the temperature field by adjusting the thermal excitation frequency. When heating with laser pulses, we can avoid the section around 5 Hz to avoid excessive temperature.

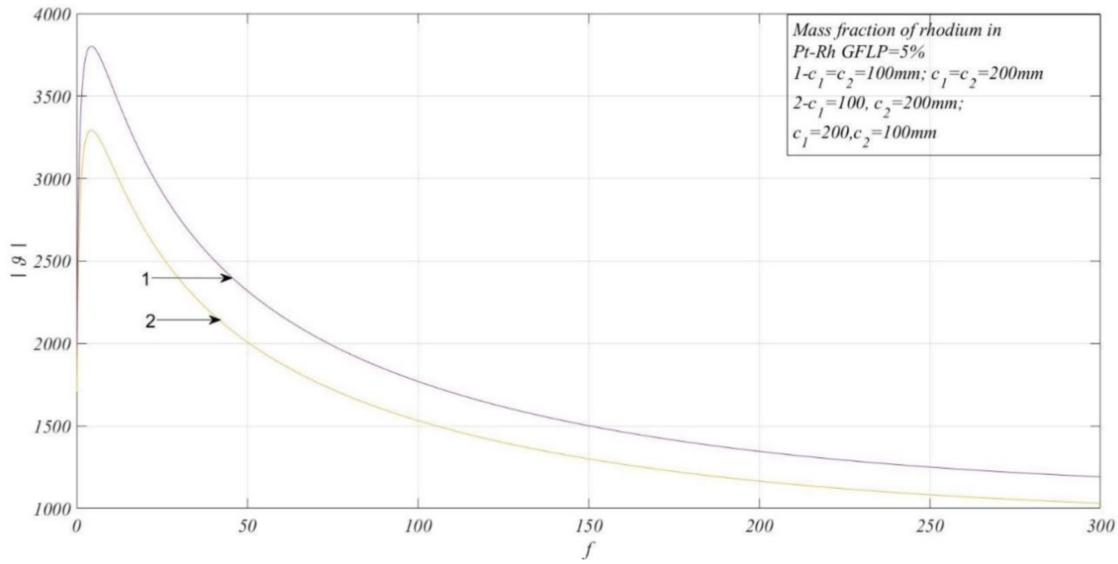

Figure 6. Temperature at the center of the circular opening of the Pt–Rh GFLP.

5. Conclusions

Based on the non-Fourier heat conduction law, this paper uses the hyperbolic thermal wave equation to study the heat propagation problem in a Pt–Rh GFLP with a circular opening. The general solution of the thermal wave scattering problem based on the heat conduction wave model is given. The variation law of temperature amplitude under various parameters is calculated, and the variation curve of temperature amplitude is given. The following conclusions can be drawn:

(1) The temperature distribution near the circular opening of the Pt–Rh GFLP is related to the position of the circular opening on the leaky plate. The specific performance is as follows: when the circular opening is located on the geometric center line, the peak temperature of the leaky plate is the highest. When the circular opening is away from the geometric center line, the peak temperature of the leaky plate is reduced, and as the offset distance increases, the peak temperature decreases more obviously.

(2) Due to the heat transfer between the Pt–Rh GFLP and the surrounding air, the temperature at the center line of the leaky plate is high. The location of the circular opening can be set to avoid overheating at the circular opening of the leaky plate due to the superposition of factors such as difficulty in heat dissipation at the center of the leaky plate and sudden temperature increase at the circular opening of the leaky plate.

(3) The temperature at the center of the circular opening of the Pt–Rh GFLP increases with the increase of the mass fraction of the rhodium element in Pt–Rh GFLP.

(4) When the laser pulse frequency is taken in the section (0 Hz, 5 Hz), the temperature at the center of the circular opening of the Pt–Rh GFLP increases with the increase of frequency. In the section (5 Hz, 300 Hz), the temperature at the center of the circular opening gradually decreases with the increase of frequency and tends to be stable. Frequency is one of the important factors affecting temperature. The influence of frequency on temperature is closely related to the thermal diffusivity of materials. Only in a certain range of thermal diffusivity can the influence of frequency on temperature work, and when it exceeds this range, it tends to be stable.

The numerical calculation results in this paper can provide theoretical support and engineering reference for the research on the temperature field of Pt–Rh GFLP under extremely rapid heating environment. The analysis of rapid heating requires going beyond Fourier's law and taking into consideration the non-vanishing relaxation time of the heat flux, as has been done in the present paper.

Author Contributions: Mainly responsible for study design work and writing manuscripts, W.J.; proposed the concept of the study and provided research methods, C.Z.; mainly responsible for data collection and analysis, Z.Y.; proposed the concept of the study, Z.S.; mainly responsible for project admission, H.J.; mainly responsible for formal analysis, B.W.; mainly responsible for literature search work and provided financial support for research, Q.W. All authors have read and agreed to the published version of the manuscript.

Funding: This research was funded by the National Natural Science Foundation of China (Grant No. 51875146), the Natural Science Foundation of Zhejiang Province of China (Grant No. LQ17E050011) and the Zhejiang Xinmiao Talents Program (Grant No. 2019R407007).

Conflicts of Interest: The authors declare no conflict of interest.

References

1. Wang, Y.Z.; Song, X.N. Dynamic model of generalized thermoelastic based on thermal mass theory. *J. Phys.* **2012**, *61*, 308–312. (In Chinese)
2. Guo, Z.Y.; Cao, B.Y. A general heat conduction law based on the concept of motion of thermal mass. *J. Phys.* **2008**, *57*, 4273–4281. (In Chinese)
3. Tian, X.G.; Shen, Y.P. Progress in the study of generalized thermo elasticity. *Adv. Mech.* **2012**, *42*, 18–28. (In Chinese)
4. Lam, T.T.; Fong, E. Application of solution structure theorem to non-Fourier heat conduction problems: Analytical approach. *Int. J. Heat Mass Transf.* **2011**, *54*, 4796–4806. [CrossRef]
5. Sarkar, D.; Haji-Sheikh, A. A view of the thermal wave behaviors in thin plates. *Int. Commun. Heat Mass Transf.* **2012**, *39*, 1009–1017. [CrossRef]
6. Yu, T.; Lan, H.; Zhi, L. Numerical Simulation of the Non-Fourier Heat Conduction in a Solid-State Laser Medium. *Chin. Phys. Lett.* **2006**, *23*, 2487–2490.
7. Barletta, A.; Zanchini, E. Unsteady Heat Conduction by Internal-energy Waves in Solids. *Phys. Rev. B* **1997**, *55*, 14208. [CrossRef]
8. Tang, D.W.; Araki, N. Non-Fourier heat conduction in a finite medium under periodic surface thermal disturbance. *Int. J. Heat Mass Transf.* **1996**, *39*, 1585–1590. [CrossRef]
9. Moosaie, A. Non-Fourier heat conduction in a finite medium subjected to arbitrary non-periodic surface disturbance. *Int. J. Heat Mass Transf.* **2008**, *35*, 376–383. [CrossRef]
10. Atefi, G.; Talaee, M.R. Non-Fourier temperature field in a solid homogeneous finite hollow cylinder. *Arch. Appl. Mech.* **2011**, *81*, 569–583. [CrossRef]
11. Mishra, S.C.; Sahai, H. Analyses of non-Fourier heat conduction in 1-D cylindrical and spherical geometry—An application of the lattice Boltzmann method. *Int. J. Heat Mass Transf.* **2012**, *55*, 7015–7023. [CrossRef]
12. Ma, X.B.; Jiang, H.Q.; Chen, D.Z. Thermal wave scattering by a cylindrical subsurface inclusion in semi-infinite slab. *Appl. Therm. Eng.* **2016**, *100*, 691–698. [CrossRef]
13. Zhang, X.Y.; Xie, Y.J.; Li, X.F. Transient thermoelastic response in a cracked strip of functionally graded materials via generalized fractional heat conduction. *Appl. Math. Model.* **2019**, *70*, 328–349. [CrossRef]
14. Niwaa, A.; Akitaa, Y.; Enomotob, K.; Aoyama, R.; Akebono, H.; Sugeta, A. High-temperature bending fatigue properties of oxide dispersion-strengthened platinum–rhodium alloy under high axial stress. *Int. J. Fatigue* **2020**, *132*, 105385. [CrossRef]
15. Sellitto, A.; Cimmelli, V.A.; Jou, D. *Mesoscopic Theories of Heat Transport in Nanosystems*; Springer: Berlin/Heidelberg, Germany, 2016.
16. Machrafi, H. *Extended Non-Equilibrium Thermodynamics: From Principles to Applications in Nanosystems*; Taylor and Francis Group: London, UK, 2019.
17. Jou, D.; Casas-Vazquez, J.; Lebon, G. *Extended Irreversible Thermodynamics*; Springer: New York, NY, USA, 2010.
18. Cimmelli, V.A. Different thermodynamic theories and different heat conduction laws. *J. Non-Equilib. Thermodyn.* **2009**, *34*, 299–333. [CrossRef]
19. Bright, T.J.; Zhang, Z.M. Common Misperceptions of the Hyperbolic Heat Equation. *J. Thermophys. Heat Transf.* **2009**, *23*, 601–607. [CrossRef]

20. Ordonez-Miranda, J.; Alvarado-Gil, J.J. Determination of thermal properties for hyperbolic heat transport using a frequency-modulated excitation source. *Int. J. Eng. Sci.* **2012**, *50*, 101–112. [CrossRef]
21. Jia, L. *Advanced Heat Transfer*; Higher Education Press: Beijing, China, 2003. (In Chinese)